32ND INTERNATIONAL COSMIC RAY CONFERENCE, BEIJING 2011

Instrument Response of the High Altitude Water Cherenkov Observatory

B. M. BAUGHMAN[1] FOR THE HAWC COLLABORATION[2]
[1]*Dept. of Physics, University of Maryland, College Park, MD 20742, USA*
[2]*For full author list see J. Goodman et al., "The HAWC Observatory", these proceedings*

bbaugh@umd.edu

DOI: 10.7529/ICRC2011/V09/0924

Abstract: The High Altitude Water Cherenkov Observatory (HAWC) is currently under construction on the slopes of Volcán Sierra Negra, Puebla, Mexico. Like its predecessor the Milagro Observatory, HAWC will have a near 100% duty cycle and large field of view (about 2 steradians). Its design substantially improves upon the gamma–hadron separation and angular resolution of the Milagro detector. We present the instrument response functions of the HAWC detector (effective area, angular resolution, energy resolution, and gamma–hadron separation) derived from detailed Monte Carlo simulations. Improvements over the performance of the Milagro Observatory are highlighted.

Keywords: hawc gamma–ray

1 Introduction

The High Altitude Water Cherenkov Observatory (HAWC) is currently under construction near Puebla, Mexico. When construction is completed in 2014 it will consist of 300 optically–isolated galvanized steel tanks, each 7.3 m in diameter and 4.5 m deep [1]. The HAWC design is built upon the successful water Cherenkov technique pioneered with Milagro [2, 3, 4, 5, 6, 7, 8, 9]. With about a factor of 10 increase in densely instrumented deep–water area over Milagro, the HAWC design provides a dramatic improvement in low–energy effective area, angular resolution, and energy resolution. The HAWC site, at an elevation of 4100 m compared to 2649 m for Milagro, extends the effective area of HAWC well below the minimum energy threshold of Milagro. The segmentation of the deep water into optically isolated tanks improves the hadron rejection efficiency over that of Milagro by a factor of about 10 at high energies. A detailed description of HAWC and its construction timeline can be found in these proceedings [1]. HAWC, with its nearly 100% duty cycle, large field of view, and large effective area, will complement the capabilities of the Fermi-LAT[10, 11, 12, 13, 14].

The instrument response functions of HAWC have been characterized using extensive CORISKA [15] and GEANT4 [16, 17] Monte Carlo simulations. Gamma rays and eight different nuclear species have been generated according to the observed abundance of cosmic rays. These simulations, which total 1.1 billion showers, have been used to characterize the instrument response of the HAWC detector.

2 Simulations

The atmospheric shower simulations for HAWC are performed in two stages. First, each primary particle and resulting shower are simulated from the top of the atmosphere to an elevation of 4100 m with CORSIKA. CORSIKA v6970 is used with QGSJET–II for high–energy hadronic interactions and FLUKA 2008.3d.1 for low–energy hadronic interactions. Second, the shower particles which survive to 4100 m are used as input for a detailed GEANT4 simulation of the HAWC detector. The simulation, which was originally developed for Milagro [18], includes detailed descriptions of the geometrical and optical properties of the HAWC tanks and photomultiplier tubes (PMTs). Particular attention has been paid to ensure that the simulation reproduces the wavelength response of the PMTs. HAWC will use the same PMTs as Milagro, and so the simulations benefit from previously constructed GEANT4 models [19].

Cosmic–ray air showers are the primary background for HAWC. A characterization of the potential to separate between gammas and hadrons (cosmic rays) with HAWC requires simulation of large quantities of cosmic–ray air showers. The number of simulated showers for each primary particle is shown in Tbl. 1. Each primary is generated with an E^{-2} energy spectrum to reduce computation time while still providing sufficient statistics at the highest energies. The events are then weighted by the spectral indices of each primary as measured by ATIC [20].

Primary	Events Generated
Gamma	255700000
Proton	776700000
Helium	113100000
Carbon	3840000
Oxygen	4000000
Neon	1950000
Magnesium	1970000
Silicon	2000000
Iron	1920000
Total	1161180000

Table 1: Generated Monte Carlo events for different primary particles.

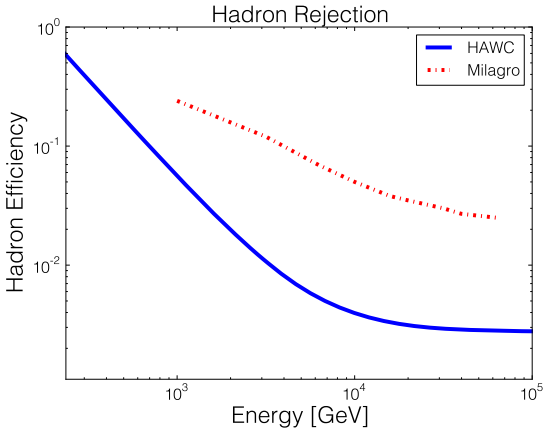

Figure 1: Comparison between hadron efficiencies of Milagro and HAWC. Gamma–ray efficiency is always $\geq 50\%$

3 Hadron Efficiency

Hadronic cosmic–ray induced air showers are morphologically different than gamma–ray induced air showers. Unlike gamma–ray showers, hadronic showers are often composed of multiple sub–showers induced by secondary particles with significant transverse momentum. These sub–showers often deposit high concentrations of energy at large distances (tens of meters) from the core of the shower. We can thereby distinguish between gamma–ray and cosmic–ray events by looking for a significant number of photo–electrons (PEs) far from the reconstructed core of the shower.

The current reconstruction algorithms used in HAWC are designed to identify showers with significant signals far from the shower core. The reconstruction algorithm identifies the PMT with the highest measured number of PEs at a radial distance of at least 40 m from the reconstructed core. This number is denoted CxPE_{40}. The air showers detected by HAWC may produce just a few PEs in several PMTs, or all 900 PMTs may measure at least one PE. Any gamma/hadron separator must scale with the size of the shower. The separator used by HAWC is:

$$S = \frac{N_{\mathrm{hit}}}{\mathrm{CxPE}_{40}} \tag{1}$$

which scales with the number of PMTs with at least one measured PE (N_{hit}). Given a fixed N_{hit}, a large value of S implies a more gamma–like shower, while a smaller S is considered to be more hadron–like.

The optimal value on which to cut S is determined by maximizing the signal to noise ratio for a given range of N_{hit} values while keeping at least 50% of the gamma rays. Events with S above the optimal value are treated as gamma rays while those below are treated as hadrons. Fig. 1 shows the resulting efficiency for hadrons to pass the optimized cut on S for a given energy. As the energy increases the efficacy of the cut improves, eliminating an increasing fraction of hadrons from observations. At the highest energies the requirement to keep 50% of gamma rays begins to dominate and thus a sub optimal cut value is used. Gamma–ray air showers at these energies often deposit large energies outside the 40 m radius. Such showers become indistinguishable using S as a gamma/hadron separator. Development is ongoing for a separator without this defect [21].

4 Effective Area

The effective area of any gamma–ray detector will depend greatly on its background rejection capability. The design of the Milagro detector made it difficult to remove the hadronic background from low energy gamma–ray samples. HAWC has been designed to avoid this problem by having a much larger deep–water area. This allows HAWC to preserve a larger fraction of its effective area at lower energies after applying the gamma/hadron cuts. Fig. 2 shows the dramatic improvement of the low–energy effective area of HAWC compared to that of Milagro, both before and after the gamma/hadron cuts have been applied. Fig. 2 shows the average vertical equivalent effective area for gamma rays incident on the detector within 30° from zenith. The effective area for HAWC were obtained using an expected background trigger rate of 16 kHz and optimal bin sizes (defined in Sec. 5). At the highest energies the gamma/hadron separator S begins to classify some gamma-ray showers as hadrons, as such the flattening of the effective area above about 30 TeV should be considered a conservative estimate. The improved low–energy response will allow HAWC to place competitive limits on transient events including GRBs [22].

5 Angular Resolution

The angular resolution of HAWC is a significant improvement over that of Milagro. This is primarily due to its larger deep–water area and the optical isolation of the detectors, which will improve the accuracy of the reconstruction of

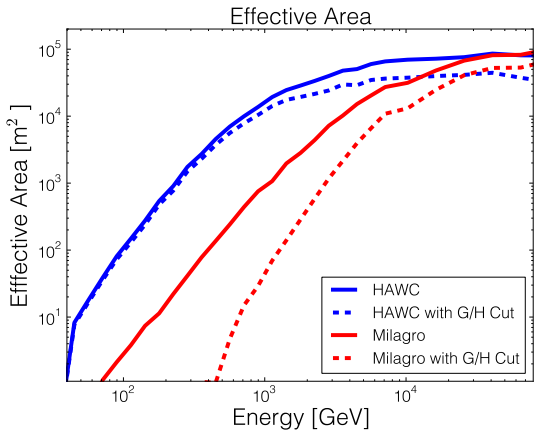

Figure 2: Comparison between Milagro and HAWC effective areas.

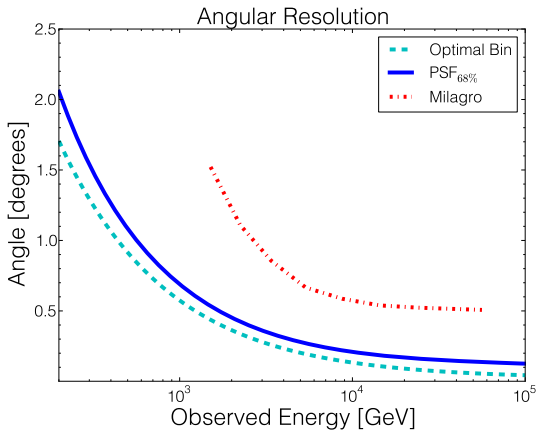

Figure 3: Comparison between Milagro and HAWC angular resolutions.

the air shower front. Reported here are two measures of the angular resolution of HAWC: the 68% containment angle ($PSF_{68\%}$) and the optimal bin size. Both methods are found using events binned in reconstructed energy. $PSF_{68\%}$ is the 68^{th} percentile of the distribution of opening angles between the true and reconstructed directions of simulated events. The optimal bin size describes the angular scale on which the signal to noise ratio is maximized for a given source and background. Here an object with a Crab–like spectrum transiting at 30° from zenith is assumed for the source. The background is assumed to be isotropic on the scale of the point spread function, as expected for a cosmic–ray background. The optimal bin size is calculated in three steps:

1. Sort the events according to the opening angle between the true and reconstructed arrival directions.
2. Calculate the cumulative distribution of the events as a function of opening angle.
3. Divide the cumulative event sum by the square root of the solid angle contained within each opening angle bin.

The maximum of this function, shown in Eqn. 2, corresponds to the angular scale on which the signal to noise ratio is optimal:

$$S/N \propto \frac{N(>\Delta\theta)}{\sqrt{2\pi \cos \Delta\theta}} \qquad (2)$$

Fig. 3 shows both $PSF_{68\%}$ and optimal bin size as well as the optimal bin size for the Milagro Observatory. The HAWC optimal bin size falls below 1° at about 500 GeV while Milagro attained a similar angular resolution only for showers at about 3 TeV. The improved angular resolution will allow HAWC to better localize sources, reduce background contamination for transient sources, and better resolve extended sources.

6 Energy Resolution

The number of PEs recorded by a water Cherenkov detector is a good estimator of the energy in an electromagnetic shower at ground level. This signal can be converted to an estimate of the energy of the primary particle, with a resolution dominated by fluctuations in the fraction of energy reaching the ground. Fig. 4 shows the energy resolution for gamma–ray induced air showers arriving well within the instrumented area of the detector and less than 45° from zenith for both HAWC and Milagro. The figure also shows the capability of HAWC to reconstruct the energy reaching the ground from a gamma–ray induced air shower to be better than 50% for primary gamma–ray energies above a few hundred GeV, labeled as 'At Ground' in the figure. The termination of the HAWC lines above about 200 TeV is due to a lack sufficient statistics to characterize the energy resolution. The resulting resolution of the primary gamma–ray energy is about 100% below 2 TeV and falls gradually with increasing energy. The resolution of the primary gamma–ray energy is a marked improvement over that of Milagro. This is the result of having a greater area of deep water, allowing HAWC to capture a larger fraction of the shower.

7 Conclusion

The HAWC design draws upon the experience accumulated during the operation of the Milagro Observatory. Located at a significantly higher altitude than Milagro, the HAWC detector will be sensitive to much lower-energy events. In addition, the altitude of 4100 m is closer to the typical altitude of shower maximum, which boosts the signals from all events and improves the resolution of the detector. The optical isolation of the HAWC tanks ensures an improved angular resolution by eliminating light leakage from individual shower particles, providing better localization of diffuse and point sources. The large deep-water area ensures that HAWC will be an excellent platform for the study of

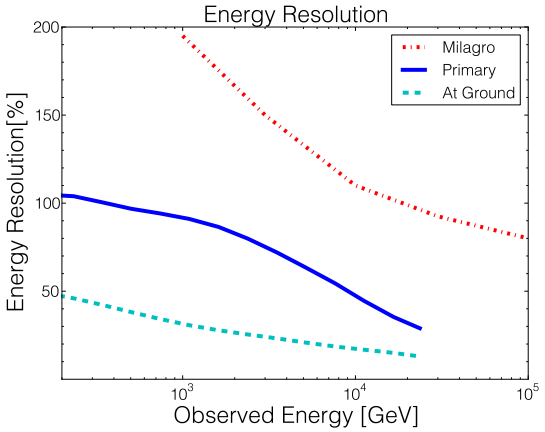

Figure 4: Comparison between Milagro and HAWC energy resolutions.

transient gamma-ray phenomena such as GRBs and flaring AGNs. With improved gamma/hadron separation, effective area, angular resolution, energy resolution, and large field of view, HAWC will provide a high–energy complement to the Fermi satellite.

References

[1] Goodman, J. A. and Braun, J. for the HAWC Collaboration. The HAWC Observatory. In *Proceedings for the 32nd International Cosmic Ray Conference* (ICRC, 2011).

[2] Milagro Collaboration. Observation of TeV gamma rays from the crab nebula with milagro using a new background rejection technique. *Astrophys. J.* **595**, 803–811 (2003). astro-ph/0305308.

[3] Atkins, R. *et al.* Constraints on very high energy Gamma-Ray emission from Gamma-Ray bursts. *Astrophys. J.* **630**, 996–1002 (2005). astro-ph/0503270.

[4] Milagro Collaboration. Evidence for TeV Gamma-Ray emission from a region of the galactic plane. *Physical Review Letters* **95** (2005). astro-ph/0502303.

[5] Abdo, A. A. *et al.* Milagro constraints on very high energy emission from Short-Duration Gamma-Ray bursts. *Astrophys. J.* **666**, 361–367 (2007). 0705.1554.

[6] Abdo, A. A. *et al.* Discovery of TeV Gamma-Ray emission from the cygnus region of the galaxy. *Astrophys. J. Lett.* **658**, L33–L36 (2007). astro-ph/0611691.

[7] Abdo, A. A. *et al.* Discovery of localized regions of excess 10-TeV cosmic rays. *Physical Review Letters* **101**, 221101+ (2008). 0801.3827.

[8] Abdo, A. A. *et al.* A measurement of the spatial distribution of diffuse TeV Gamma-Ray emission from the galactic plane with milagro. *Astrophys. J.* **688**, 1078–1083 (2008). 0805.0417.

[9] Abdo, A. A. *et al.* The Large-Scale Cosmic-Ray anisotropy as observed with milagro. *The Astrophysical Journal* **698**, 2121+ (2009).

[10] Abdo, A. A. *et al.* Fermi/Large area telescope bright Gamma-Ray source list. *Astrophys. J. Supp.* **183**, 46–66 (2009). 0902.1340.

[11] Abdo, A. A. *et al.* The on-orbit calibration of the fermi large area telescope. *Astroparticle Physics* **32**, 193–219 (2009). 0904.2226.

[12] Abdo, A. A. *et al.* The first fermi large area telescope catalog of gamma-ray pulsars. *Astrophys. J. Supp.* **187**, 460–494 (2010). 0910.1608.

[13] Abdo, A. A. *et al.* The first catalog of active galactic nuclei detected by the fermi large area telescope. *Astrophys. J.* **715**, 429–457 (2010). 1002.0150.

[14] Abdo, A. A. *et al.* Fermi large area telescope first source catalog. *Astrophys. J. Supp.* **188**, 405–436 (2010). 1002.2280.

[15] Heck, D., Knapp, J., Capdevielle, J. N., Schatz, G. & Thouw, T. Corsika: A monte carlo code to simulate extensive air showers. Report FZKA 6019, Institut für Kernphysik Forschungszentrum (1998).

[16] Geant4 Collaboration *et al.* Geant4-a simulation toolkit. *Nuclear Instruments and Methods in Physics Research A* **506**, 250–303 (2003).

[17] Allison, J. *et al.* Geant4 developments and applications. *IEEE Transactions on Nuclear Science* **53**, 270–278 (2006).

[18] Vasileiou, V. for the Milagro Collaboration. Monte carlo simulation of the milagro gamma-ray observatory. In *International Cosmic Ray Conference*, vol. 3 of *International Cosmic Ray Conference*, 1377–1380 (2008).

[19] Vasileiou, V., Ellsworth, R. W. & Smith, A. Photocathode-Uniformity tests of the hamamatsu r5912 photomultiplier tubes used in the milagro experiment. In *International Cosmic Ray Conference*, vol. 4 of *International Cosmic Ray Conference*, 813–816 (2008). 0711.1910.

[20] Panov, A. D. *et al.* Energy spectra of abundant nuclei of primary cosmic rays from the data of ATIC-2 experiment: Final results. *Bulletin of the Russian Academy of Science, Phys.* **73**, 564–567 (2009). 1101.3246.

[21] Grabski, V. for the HAWC Collaboration. Gamma/hadron separation study for the HAWC detector on the basis of the multidimensional feature space using non parametric approach. In *Proceedings for the 32nd International Cosmic Ray Conference* (ICRC, 2011).

[22] Taboada, I. for the HAWC Collaboration. Sensitivity of HAWC to GRBs. In *Proceedings for the 32nd International Cosmic Ray Conference* (ICRC, 2011).